Convergent evolution of tertiary structure in rhodopsin visual proteins from vertebrates and box jellyfish

Elliot Gerrard[a,1], Eshita Mutt[b,1], Takashi Nagata[c], Mitsumasa Koyanagi[c], Tilman Flock[b,d], Elena Lesca[b,d], Gebhard F. X. Schertler[b,d], Akihisa Terakita[c,2], Xavier Deupi[b,2], and Robert J. Lucas[a,2]

[a]Faculty of Biology Medicine and Health, University of Manchester, Manchester M13 9PL, United Kingdom; [b]Paul Scherrer Institute, 5232 Villigen PSI, Switzerland; [c]Department of Biology and Geosciences, Graduate School of Science, Osaka City University, 558-8585 Osaka, Japan; and [d]Department of Biology, ETH Zürich, 8093 Zurich, Switzerland

Edited by Thomas P. Sakmar, Rockefeller University, New York, NY, and accepted by Editorial Board Member Jeremy Nathans April 26, 2018 (received for review December 8, 2017)

Box jellyfish and vertebrates are separated by >500 million years of evolution yet have structurally analogous lens eyes that employ rhodopsin photopigments for vision. All opsins possess a negatively charged residue—the counterion—to maintain visible-light sensitivity and facilitate photoisomerization of their retinaldehyde chromophore. In vertebrate rhodopsins, the molecular evolution of the counterion position—from a highly conserved distal location in the second extracellular loop (E181) to a proximal location in the third transmembrane helix (E113)—is established as a key driver of higher fidelity photoreception. Here, we use computational biology and heterologous action spectroscopy to determine whether the appearance of the advanced visual apparatus in box jellyfish was also accompanied by changes in the opsin tertiary structure. We found that the counterion in an opsin from the lens eye of the box jellyfish *Carybdea rastonii* (JellyOp) has also moved to a unique proximal location within the transmembrane bundle—E94 in TM2. Furthermore, we reveal that this Schiff base/counterion system includes an additional positive charge—R186—that has coevolved with E94 to functionally separate E94 and E181 in the chromophore-binding pocket of JellyOp. By engineering this pocket—neutralizing R186 and E94, or swapping E94 with the vertebrate counterion E113—we can recreate versions of the invertebrate and vertebrate counterion systems, respectively, supporting a relatively similar overall architecture in this region of animal opsins. In summary, our data establish the third only counterion site in animal opsins and reveal convergent evolution of tertiary structure in opsins from distantly related species with advanced visual systems.

opsin | counterion | G-protein–coupled receptors | vision | evolution

Opsins are G-protein–coupled receptors that bind covalently a light-sensitive ligand, the chromophore retinaldehyde. These proteins mediate vision throughout the animal kingdom and have been employed for optogenetic manipulation of G-protein–mediated signaling cascades (1, 2). Light absorption triggers a *cis*-to-*trans* isomerization of the chromophore, which in turn causes conformational changes in the receptor that uncover a cytoplasmic G-protein binding site. Free retinaldehyde is maximally sensitive to UV light but is shifted to preferring lower-energy, visible, wavelengths through protonation of the covalent bond that anchors it to the opsin [forming a protonated Schiff base (PSB)]. One of the most important structural features of opsins is an acidic residue—the "counterion"—positioned near to the chromophore to stabilize the PSB at physiological pH, thus ensuring visible-light sensitivity (3, 4).

The location of this counterion in the second extracellular loop [E181 (5)] is highly conserved among opsins. It is currently thought to have moved only once during evolution, in the ancestor of vertebrate visual opsins (members of the ciliary-type opsin clade that include rod and cone opsins), to a site in the transmembrane bundle [E113 (6–8)] closer to the chromophore. This counterion displacement is a defining structural feature of vertebrate visual opsins and acts as a mechanism for maximizing light-driven conformational changes and enhancing G-protein activation (9).

The most basal divide in the animal kingdom is between radially and bilaterally symmetrical organisms. Opsins exist in extant members of both, but all of the structural information for metazoan opsins comes from bilateria. A parsimonious prediction is that opsins from radiata employ the same counterion (E181) as the basal bilatarian opsin, and indeed sequence alignments reveal widespread appearance of a glutamate residue at this position (10). However, vertebrate visual opsins also have a glutamate at this site (11), indicating that the mere presence of a negatively charged residue at this location is insufficient to infer counterion function. Moreover, radiata have had just as long as bilataria to evolve structural modifications in their opsins. In general, visual structures in radiata lack the complexity found in many bilatarian species. However, one group, the box jellyfish (phylum, Cnidaria; order, Cubozoa) have developed lens eyes and advanced visual responses (12–15). Thus, evolution of cubozoan vision recapitulates some of the features of vertebrate visual systems.

Here, we set out initially to determine whether E181 acts as the counterion in a representative opsin from the radiata. For this purpose, we chose JellyOp, a visible-light–sensitive opsin from the box jellyfish *Carybdea rastonii* (16). JellyOp is expressed in the upper and lower lens eyes of this organism and has been applied as an optogenetic tool to provide light-driven activation

Significance

Complex photoreceptors have independently evolved in animals with radial and bilateral symmetry, but little is known about the proteins that transduce light information (opsins) in radially symmetrical animals. We use homology modeling and heterologous action spectroscopy to study the structure of an opsin (JellyOp) from the lens eye of the visually competent box jellyfish, *Carybdea rastonii*. We find that a key structural feature of animal opsins—the counterion—maintains visible-light sensitivity in JellyOp from a unique location, E94 in the transmembrane bundle. This unique position for the counterion, the third only discovered in animal opsins, closely mirrors the location in vertebrate visual proteins, which was thought to be a unique adaptation in vertebrates to achieve higher fidelity photoreception.

Author contributions: E.G., E.M., T.N., G.F.X.S., A.T., X.D., and R.J.L. conceived the study; E.G., E.M., G.F.X.S., A.T., X.D., and R.J.L. designed research; E.G., E.M., T.N., and X.D. performed research; E.M., E.L., T.F., M.K., and X.D. performed computational and evolutionary modeling; E.G., E.M., T.N., M.K., T.F., E.L., A.T., and X.D. analyzed data; and E.G., E.M., A.T., X.D., and R.J.L. wrote the paper.

The authors declare no conflict of interest.

This article is a PNAS Direct Submission. T.P.S. is a guest editor invited by the Editorial Board.

[1]E.G. and E.M. contributed equally to this work.

[2]To whom correspondence may be addressed. Email: terakita@sci.osaka-cu.ac.jp, xavier.deupi@psi.ch, or robert.lucas@manchester.ac.uk.

This article contains supporting information online at www.pnas.org/lookup/suppl/doi:10.1073/pnas.1721333115/-/DCSupplemental.

Published online May 23, 2018.

of Gαs signaling with high sensitivity and signal:noise (16–18). JellyOp thus represents a good system to explore the evolution of the position of the counterion along the development of complex visual structures in radiata, and also to gain structural information on the retinal-binding site that could facilitate rational engineering of improved optogenetic tools.

Results

JellyOp Does Not Utilize Either of the Two Established Counterion Positions, 113 or 181. JellyOp is found in the upper and lower lens eyes of box jellyfish *C. rastonii* (16), a member of the Cnidaria phylum of radially symmetrical animals (Fig. 1 *A* and *B*). JellyOp's sequence includes a glutamic acid at position 181 (bovine rhodopsin numbering system; 152 in JellyOp; *SI Appendix*, Table S1) found to be the primary counterion in squid and amphioxus retinal-binding proteins (5) and, due to its conservation across the opsin family, presumed to be the ancestral counterion of all animal opsins (9). We therefore started by determining whether E181 was JellyOp's counterion by assessing the impact of replacing it with a neutral residue. Removal of a counterion should reduce the pK_a of the PSB and shift the pigment to UV light sensitivity at neutral pH (5, 6). However, spectroscopy of a purified E181Q mutant of JellyOp did not produce the expected shift in absorption maximum or pK_a (Fig. 1 *C* and *D*). These data suggest that E181 is not JellyOp's counterion and, given that JellyOp lacks a negative charge at the equivalent position of site 113 in vertebrate rhodopsin (*SI Appendix*, Fig. S1), that this pigment utilizes a unique counterion position.

JellyOp Utilizes a Unique Position, E94 in TM2, as Its Primary Counterion. To identify this potential unique counterion residue, we built a 3D homology model of JellyOp (*Materials and Methods*). The model predicted that, in addition to E181, another glutamate residue, E94, would be located in the retinal-binding pocket close to the Schiff base (Fig. 1*E*). Encouragingly, a survey of opsin sequences revealed that this residue was also present in opsins from other cnidarian species (*SI Appendix*, Fig. S1). Molecular dynamics simulations performed on our model (*Materials and Methods*) suggested that a salt bridge between E94 and the PSB is structurally feasible and stable (*SI Appendix*, Fig. S3). To explore the possibility of E94 serving as JellyOp's counterion, we attempted UV-visible spectroscopy of an E94Q mutant. However, we were unable to obtain active protein after purification (Fig. 1*F* and *SI Appendix*, Fig. S2).

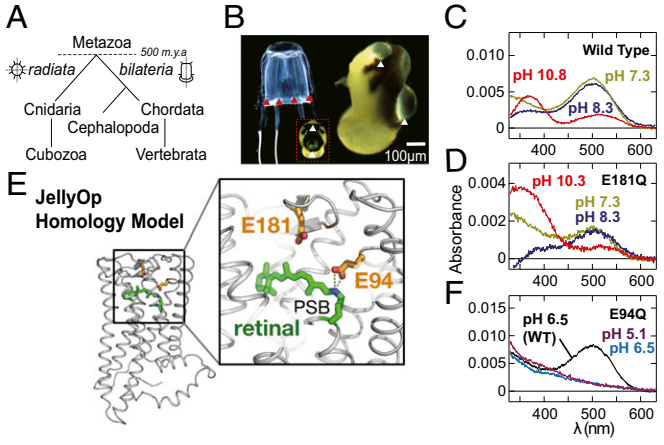

Fig. 1. Box jellyfish opsin does not utilize the ancestral counterion position, E181. (*A*) Schematic of the phylogenetic relationship between the three metazoan groups to have evolved lens eyes (cubozoa, cephalapoda, and vertebrata) and their common ancestor preceding the split of radial and bilateral animals ~500 Mya. (*B*) Box jellyfish *C. rastonii* (*Left*), with the sensory apparatus (rophalium) indicated by red arrows and *Inset*; side view of a rophalium (*Right*) in which JellyOp is found in the upper and lower lens eyes (white triangles). (*C* and *D*) UV-visible light spectroscopy of purified wild type (*C*) and E181 (*D*) mutants of JellyOp reconstituted with 11-*cis* retinal; the red trace indicates the pH at which the majority of the Schiff base was converted from the protonated to deprotonated form. (*E*) Three-dimensional structural model of JellyOp, showing the location of E181 in the second extracellular loop and an additional glutamate residue (E94) in a suitable position to act as a counterion to the PSB. (*F*) UV–visible-light spectroscopy of the purified JellyOp E94Q mutant presented with 11-*cis* retinal did not reveal a peak in absorption in either UV or visible regions of the spectrum. Dark-minus-light difference spectra with crude extract also did not exhibit any obvious peak (*SI Appendix*, Fig. S2), indicating that the purified protein mutant failed to bind the chromophore.

Problems with efficient expression and purification of opsin pigments and mutants thereof are a common roadblock to their structural and biophysical characterization. Therefore, we sought an alternative method to screen for counterion neutralization. JellyOp expresses efficiently in HEK293 cells and upon light activation causes a robust induction of cAMP through activation of the Gαs pathway that can be tracked in live cells with a luminescent cAMP reporter (Fig. 2*A*) (16–18). We therefore attempted to use the relative spectral sensitivity of the JellyOp-driven second messenger response (action spectrum) to test the hypothesis that the E94Q substitution had resulted in counterion neutralization. Encouragingly, light-driven increases in cAMP could be elicited in HEK293 cells expressing E181Q and E94Q versions of JellyOp but were absent in cells lacking opsin (Fig. 2*A*).

We started by attempting to recreate our finding with the E181Q mutant using this technique. To this end, we described the irradiance dependence of cAMP reporter bioluminescence for eight near-monochromatic stimuli (between 365 and 595 nm) in cells expressing wild-type or E181Q mutant JellyOp (Fig. 2*B*). From resultant irradiance response curves, we were able to describe the spectral efficiency of the pigment by plotting relative sensitivity as a function of stimulus wavelength (Fig. 2 *C* and *D*). These data could then be fit with the template of an opsin:retinaldehyde pigment [modified Govardovskii nomogram; *Materials and Methods* (19)] to estimate the expressed pigment's peak sensitivity [λ_{max}; as previously (20)]. Our wild-type JellyOp action spectrum was best described by a pigment template with $\lambda_{max} = 498$ nm ($R^2 = 0.97$, $n = 6$; Fig. 2*C*), similar to that previously reported for JellyOp from spectroscopy (16). The spectral sensitivity of the E181Q mutant determined with this technique ($\lambda_{max} = 495$ nm, $R^2 = 0.88$, $n = 6$; Fig. 2*D*) was similar to that recorded using spectroscopy and lacked a detectable shift to UV sensitivity (Fig. 1*D*), consistent with the conclusion that E181 does not serve as JellyOp's counterion.

Turning to the E94Q mutant, we found that it supported robust light-dependent increases in cAMP when expressed in HEK293 cells (Fig. 2*A*), indicating that our failure to purify sufficient active pigment for absorbance spectroscopy could be overcome with this in-cell approach. The E94Q mutant did not behave like a single pigment, in which the principle of univariance holds that the slope and saturation point of irradiance response curves should be similar at all wavelengths. Rather, the saturating amplitude of responses driven by JellyOp E94Q was significantly different at UV vs. visible wavelengths (max fold-baseline increase in cAMP following 2-s light pulse; 30.9 ± 1 vs. 107.6 ± 2.5, 470 vs. 365 nm, $n = 4$, $P < 0.001$; Fig. 2*E*), indicating that this pigment must exist in at least two functionally distinct conformations sensitive to different portions of the spectrum.

We reasoned that the failure of univariance for the JellyOp E94Q light response could arise from elimination of a counterion, as the consequent reduction in pK_a of the Schiff base is known to produce an equilibrium of protonated and deprotonated pigment states at physiological pH (5, 6). Such equilibrium would produce two spectrally distinct pigments, one sensitive to UV and the other to visible light. The action spectrum of JellyOp E94Q (Fig. 2 *F* and *G*) confirmed that was indeed the case. In agreement with the hypothesis that this mutant lacked a counterion, the action spectrum showed maximal sensitivity to UV light, indicating appearance of a pigment with a deprotonated Schiff base [predicted $\lambda_{max} = 380$ nm (6)]. However, sensitivity at longer wavelengths was too high to be explained by a single UV-sensitive pigment (Fig. 2*G*), revealing that a visible-light–sensitive pigment with a

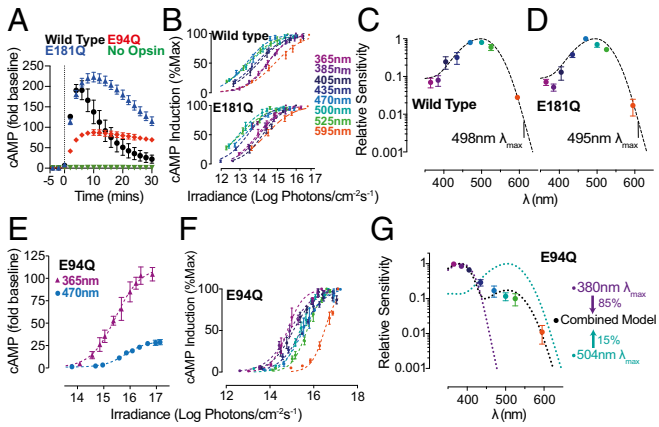

Fig. 2. Spectral sensitivity of JellyOp putative counterion mutants in HEK293 cells. (*A*) Time course of light-dependent cAMP induction [fold change in luminescence = raw luminescence units (RLU)/mean RLU over baseline before light exposure] in HEK293 cells expressing either wild type, E181Q, E94Q JellyOp, or no opsin, following a light pulse (λ_{max} = 470 nm, 2 s, ~1 mW/cm^{-2}) at time = 0 (dotted line; n = 4 experiments, mean of 3 wells per experiment). (*B*) Irradiance response curves at eight narrow-wavelength bands for peak change in luminescence (normalized to maximum response across all wavelengths and irradiances) for wild-type (*Top*) and E181Q mutant (*Bottom*) JellyOp in response to 500-ms light pulse (n = 6 experiments). (*C* and *D*) Action spectra derived from these irradiance response curves fitted with Govardovskii visual templates using sum of squares method to determine best fit λ_{max} (498 and 495 nm for wild type and E181Q, respectively). (*E*) Irradiance response curves for cAMP induction (fold change in reporter luminescence from baseline) in HEK293 cells expressing E94Q JellyOp mutant exposed to 500-ms flashes of UV (365 nm, purple) or visible (470 nm, blue) light (n = 6 experiments, 1 replicate per experiment). (*F*) Normalized irradiance response curves for HEK293 cells expressing E94Q JellyOp mutant (light pulse, 500 ms; n = 6 experiments) at eight narrow-wavelength bands (normalized to maximum response at that wavelength). (*G*) Action spectrum for the E94Q mutant light response with nomograms for the predicted absorbance spectrum for a deprotonated Shiff base (λ_{max} = 380 nm; blue dotted line) and the best fit for the long wavelength limb of the action spectrum (λ_{max} = 504 nm; purple dotted line) shown as a reference. The data could be approximated by a composite spectrum (black dotted line) produced as a linear sum of these two nomograms weighted 85:15 in favor of the UV pigment (shown at *Right* in schematic form).

protonated Schiff base must also be present. To estimate the λ_{max} of this latter pigment, we fitted a separate nomogram to the longer wavelength portion of the action spectrum (470–595 nm), over which responses could not practically emanate from a pigment with a UV λ_{max} at the range of light intensity used. This revealed a good fit for an opsin template with λ_{max} = 504 nm (*SI Appendix*, Fig. S4). Subsequently, we found that the whole E94Q action spectrum could now be accurately predicted by the combined spectral sensitivity of an opsin existing in deprotonated (λ_{max} = 380 nm) and protonated (λ_{max} = 504 nm) Schiff base states at an 85:15 ratio (R^2 = 0.95, n = 6; Fig. 2*G*).

Evolution of the Counterion Position. Several phylogenetic studies agree that cnidarian opsins ("cnidopsins") share the largest degree of homology with ciliary opsins, forming a superclade that diverged after the two other major opsin clades; the rhabdomeric-type and the group 4 opsins (10, 22–24). The discovery of a unique counterion position within the cnidopsin clade led us to wonder at what point in evolution this unique position appeared and whether it challenges the current status of E181 as the ancestral counterion position in all animal opsin clades (25). To address this question, we employed ancestral sequence reconstruction techniques to estimate the residue composition of the three known counterion positions—E94, E113, and E181—over the course of animal opsin evolution (*Materials and Methods*) (21, 26–28). A tree built from an alignment of 141 animal opsin sequences (*SI Appendix*, Table S2) recovered the previously described phylogenetic relationship between the four clades, positioning the cnidopsins group as a sister group to ciliary opsins (Fig. 3*A*). At the internal node representing the last common ancestor of the ciliary and cnidarian opsins (node C, Fig. 3*A*), we looked for the most likely amino acid present at the three counterion positions. Consistent with current opinion, our analysis showed that E181 was extremely likely to be present (0.99 probability; Fig. 3*B*; see *SI Appendix*, Table S3 for supporting statistical likelihoods), whereas neither E94 nor E113 were likely to be present in this common ancestor (<0.001 probability). E181 was also present in the common ancestral sequence of all four opsin clades and in the common ancestor of the rhabdomeric and group 4 lineages (nodes A and B, both >0.98 probability; Fig. 3 *A* and *B*). These data suggest that the common ancestor of ciliary and cnidarian opsins was very unlikely to have a proximal counterion at positions 94 or 113.

Looking closely at the cnidopsin lineage, we found that a glutamic acid became conserved at position 94 between ancestral nodes F (0.004 probability) and G (0.942 probability) (Fig. 3 *A* and *B* and *SI Appendix*, Table S2). Subsequently, all extant cnidarian opsins found after ancestor G, which include selected opsins from cubozoans *Tripedalia cystophora* and *C. rastonii*, but also hydras *Hydra magnipapillata*, *Podocoryne carnea*, and *Cladonema radiatum*, possess a glutamic acid at position 94 (*SI Appendix*, Fig. S1). These data suggest that counterion displacement to position 94 occurred before the hydra-cubozoa split within the cnidarian phylum. These data also confirm that the counterion displacement observed in JellyOp is unique to the cnidopsin clade, occurring independently to the counterion displacement observed in ciliary visual opsins found in vertebrates at position 113, at which a glutamic acid became conserved between nodes D (probability 0.001) and E (probability 0.999).

Counterion Displacement from E181 to E94 in JellyOp Is Facilitated by R186. It appears then that E94 is a counterion unique to cnidarian opsins. JellyOp, however, like ciliary visual opsins, retains a glutamic acid at the ancestral counterion position, 181 (Fig. 3*B*), located in the second extracellular loop of the receptor. One may then ask whether this single site change was sufficient to displace the counterion from E181 in the cnidopsins, or whether some

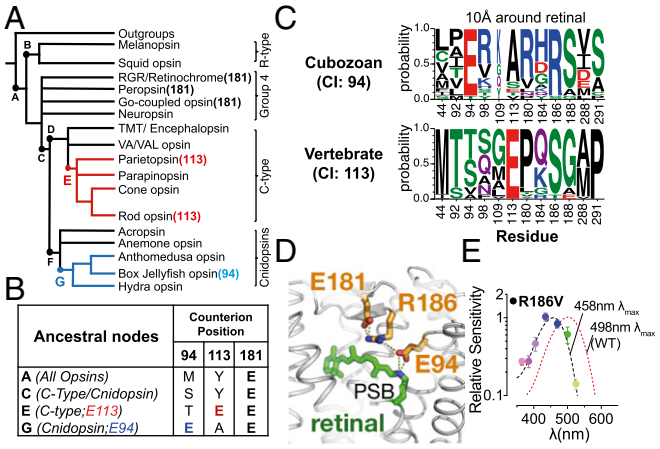

Fig. 3. E94 and R186 are unique to the cnidopsins clade of animal opsins. (*A*) Schematic depiction of the maximum-likelihood phylogenetic tree calculated for our ancestral opsin sequence dataset. Ancestral opsin sequences were reconstructed at nodes A–G and the most likely amino acid constituent at the three counterion positions (94, 113, 181) are shown in table form for selected ancestors below (*B*). (*C*) Sequence variability in the retinal binding pocket of cnidopsins containing E94 (*Top*) and vertebrate containing E113 (*Bottom*) opsins (size of letter depicts frequency across opsins from that group). (*D*) Structural model of JellyOp's chromophore binding site showing the location of the R186 residue between E181, E94, and the PSB. (*E*) Action spectrum for cAMP induction in HEK293 cells expressing R157V mutant of JellyOp with best-fit opsin nomogram (λ_{max} = 458 nm; dotted black line; n = 6 experiments, 1 replicate per experiment; data are mean ± SEM relative sensitivity at that wavelength). The spectral sensitivity of wild-type JellyOp (λ_{max} = 498 nm) is shown for comparison.

other modification in the receptor is required to stop E181 from performing this function. To address the environment of the retinal-binding pocket in JellyOp, we looked for additional features unique to cubozoan opsins. To do so, we first analyzed the sequence composition in the binding pocket across animal opsins (*Materials and Methods*). This identified a highly conserved arginine at position 186 as a unique feature of cubozoan opsins containing E94 (Fig. 3*C*). Furthermore, our structural model of JellyOp suggests that the positively charged R186 sits between the two acidic residues E181 and E94 (Fig. 3*D*) and could therefore play a role in determining the active counterion for this protein by restraining E181 away from the Schiff base. Molecular dynamic simulations support the hypothesis that R186 primarily interacts with E181 inside JellyOp's retinal binding pocket (*SI Appendix*, Fig. S3). To explore this possibility, we constructed an action spectrum for an R186V mutant of JellyOp under heterologous expression in HEK293 cells. This revealed a large (43-nm) blue shift in spectral sensitivity ($\lambda_{max} = 458$ nm, $R^2 = 0.9$, $n = 6$; Fig. 3*E*), suggesting a decrease in electron delocalization along the retinal chain (29). Given the nonpolar nature of the valine introduced at position 186, we hypothesize that E181—in the absence of R186—is able to interact with the Schiff base to cause a hyposochromatic shift in spectral sensitivity.

Proximal or Distal Counterions Can Be Employed in JellyOp. Having determined this unique structural organization by which JellyOp has achieved functional separation of E181 and E94, we compared the likely 3D organization of residues 94, 113, 181, and 186 in ancestral and extant pigments to infer the likely counterion systems that have evolved over time. We did this by threading the statistically inferred sequence of ancestor A (all opsins, Fig. 3*A*) through the squid rhodopsin crystal structure template using homology modeling tools (*Materials and Methods*). This revealed that the glutamate residue at position 181 was most likely located at a distal position in the extracellular domains of the receptor at ~6 Å from the PSB in ancestor A (Fig. 4*A*), in a similar manner to the crystal structure of squid rhodopsin (Fig. 4*B*)—representative of R-type opsins. These distal counterion systems probably require a bridging network of water molecules to interact with the PSB, as proposed for squid rhodopsin (30). On the other hand, both the ciliary and cnidopsin counterions (at positions 113 and 94, respectively) reside in the transmembrane bundle of the receptor, placing a proximal acidic functional group at ~3 Å from the PSB (Fig. 4 *C* and *D*). The R186 positive charge is retained and unique to the cnidopsin E94-containing common ancestor (*SI Appendix*, Table S3). This relocation of the counterion from a distal to a proximal position relative to the Schiff base in ciliary and cnidarian opsins shows a high degree of structural homology despite evolving in separate opsin lineages.

We then wondered whether the presence of both R186 and E94 was sufficient to displace the counterion from E181 to E94, as might be predicted to have occurred during the evolution of cnidopsins. To try to recover E181 as a functional counterion in JellyOp, we removed the R186 charge from the E94Q mutant, in the expectation that this would free E181 to act as a counterion (Fig. 4*E*). We found that this double mutation (E94Q/R186V) rescued a significant proportion of visible-light–sensitive pigment ($\lambda_{max} = 380$ and 508 nm, 15:85 ratio, $R^2 = 0.95$, $n = 6$; Fig. 4*F*). Neutralizing both E181 and E94 resulted in a maximally UV-sensitive pigment, although a portion of visible-light–sensitive pigment still remained (*SI Appendix*, Fig. S5). These results indicate that E181 is able to adequately maintain visible-light sensitivity in the E94Q/R186V mutant, suggesting that E94 could have been acquired from an ancestor with E181 via relatively few amino acid substitutions.

Given the high degree of structural homology between the vertebrate and cnidopsin counterions, we also asked whether JellyOp was capable of utilizing the ciliary counterion position, E113, to maintain visible-light sensitivity. Introduction of the

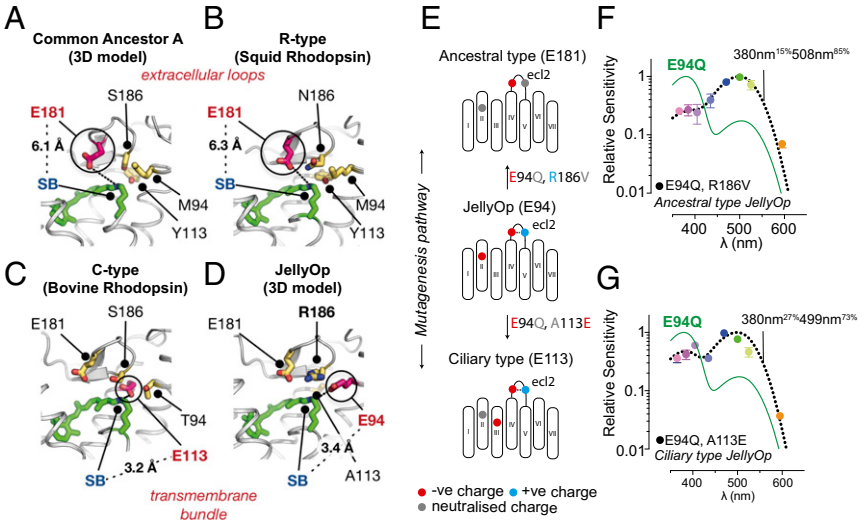

Fig. 4. Proximal and distal counterion phenotypes. (*A* and *B*) Three-dimensional structure of retinal binding pockets featuring a distal counterion: the common ancestor A (3D model; *Materials and Methods*) and R-type opsins (e.g., squid rhodopsin; PDB ID 2Z73). (*C* and *D*) Three-dimensional structure of retinal binding pockets featuring a proximal counterion: C-type vertebrate opsins (e.g., bovine rhodopsin; PDB ID code 1GZM) and cnidopsins (JellyOp model; *Materials and Methods*). Likely active counterions are circled, and their distance to the PSB is displayed. (*E*) Schematic of the residue changes (mutagenesis pathway) required to generate versions of JellyOp's in which the counterion is translocated from its actual position in the second transmembrane helix (*Middle*; E94, cubozoan type) to the site of the vertebrate counterion (E113) in the third transmembrane helix (*Bottom*; E94Q/A113E) or that of the ancestral opsin in the second extracellular loop (E181) by removing the R186-lock residue (*Top*; E94Q/R186V). (*F* and *G*) Action spectra for cAMP responses in HEK293 cells expressing E94Q/R186V or E94Q/A113E mutants (*F* and *G*, respectively). The spectral sensitivity profile of the E94Q mutant is shown for reference (solid green line). In each case, the double mutant shows enhanced visible-light sensitivity indicative of increased PSB stability. The relative fraction of pigment in the protonated state is estimated by fitting the action spectrum with a composite sensitivity function as the weighted sum of the nomogram for a deprotonated Schiff base ($\lambda_{max} = 380$ nm) and a visible pigment ($\lambda_{max} = 498$ and 508 nm for E94Q/A113E and E94Q/R186V mutants, respectively). The optimal weighting for the visible-light–sensitive (PSB) pigment was 73% and 85% for pigments with accessible glutamate residues at sites 113 and 181, respectively, in contrast to 15% for the E94Q mutant alone (green). $n = 6$ experiments, 1 replicate per experiment; data are mean ± SEM.

ciliary rhodopsin counterion into the E94Q mutant of JellyOp (E94Q/A113E) again increased the proportion of protonated, visible-light–sensitive pigment (λ_{max} = 380 and 499 nm, 27:73 ratio, $R^2 = 0.67$, $n = 6$; Fig. 4*G*), indicative of an increase in PSB stability. These data in JellyOp demonstrate the functional redundancy of the ciliary and cnidarian counterion positions, supporting the hypothesis that the two counterion positions evolved independently to perform the same function.

Discussion

In this study, we have revealed that JellyOp utilizes E94 in the second transmembrane helix to maintain visible-light sensitivity at physiological pH by acting as counterion to the PSB. In doing so, we have established the first non-ciliary opsin with a proximal counterion. Our ancestral sequence reconstruction analysis and mutagenesis experiments indicate that, like the vertebrate E113 counterion, E94 most likely evolved from an ancestor with E181, reinforcing the view of E181 as the ancestral counterion of all animal opsins. Thus, our data represent only the second documented occasion that the counterion has moved over the course of opsin evolution. Given the detrimental effect to opsin function of disrupting the counterion, it is perhaps not surprising that major changes in its position within the opsin structure are so rare. It is notable, however, that on both occasions the counterion has displaced from a distal to a proximal location, relative to the Schiff base. The selective advantage of this structural change has been established for vertebrate rhodopsins, in which the displacement of the counterion to E113 allows the formation of an extended hydrogen-bonding network involving E181 that amplifies the light-induced conformational changes in transmembrane helices 5 and 6 (31) and increases G-protein activation efficiency (25). While it remains to be determined whether the counterion displacement performs a similar function for JellyOp, it does appear to possess a similar architecture of the retinal-binding pocket to that of ciliary rhodopsins (with the ancestral E181 in a distal position in the second extracellular loop and an additional proximal acidic residue in the transmembrane bundle acting as counterion). Supporting this hypothesis, our structural model of JellyOp places E94 in the second transmembrane helix, facing the chromophore-binding pocket, and at ∼3.4 Å of the PSB (Fig. 4 *C* and *D*). The hypothesis that E113 and E94 perform the same role by occupying "functionally equivalent" locations in the chromophore-binding pocket is supported by our engineering of JellyOp, showing that glutamate residues at sites 94 and 113 are at least partly interchangeable for PSB stabilization.

Convergent evolution is a widespread biological phenomenon that has been observed on scales ranging from animal behavior to protein structure (33, 34). The appearance of E94 and E113 in cnidopsin and ciliary opsin branches meets several of the criteria for categorization as an instance of convergent evolution. First, our evolutionary analysis indicates that the two proximal counterions arose independently in ancestral opsins within the cnidopsins and ciliary opsin clades. Second, given the scarcity of counterion displacements in animal opsins, it is most unlikely that these events were functionally neutral chance events. Rather, our structural model indicates that they had a similar effect on a critical aspect of opsin tertiary structure—bringing the counterion from a distal location in the extracellular loops into a proximal position in the transmembrane bundle close to the PSB. Furthermore, our mutagenesis experiments indicate that either position can house a counterion in JellyOp, demonstrating some degree of functional redundancy. Whether the cnidarian E94 counterion imparts the same effect on G-protein activation efficiency as the vertebrate E113 counterion remains to be demonstrated; this would provide further evidence that the two counterions have evolved convergently.

Our study further identifies an arginine at position 186 as critical for the counterion displacement in JellyOp. Whereas E181 has been shown to interact with the Schiff base in the active state of vertebrate ciliary opsins (35) and even act as a synergistic counterion with E113 in a recently described tunicate opsin (36), R186 appears to isolate E181 from the PSB of JellyOp, inhibiting its ability to act as a counterion. It follows that the evolution of cubozoan opsins was characterized by accumulation of both E94 and R186. In vertebrates, which do not appear to have an equivalent of R186, the existence of a UV-sensitive, counterionless, intermediate has been proposed as an intermediate step in the counterion displacement (9). If the JellyOp ancestor acquired E94 before R186, then the equivalent two-step counterion displacement could have occurred without a UV-sensitive stage. The presence of this additional unique mechanism is an argument to suggest that if these two counterion displacements are to be considered convergent events, they have occurred through nonsynonymous mechanisms. An example of this has been recently demonstrated in the acquisition of thermal stability in Andean catfish rhodopsins (33).

Comparative sequence analysis suggests that the E94 counterion is not restricted to JellyOp but is present also in other cubozoan visual proteins. E94 is found in opsin sequences from at least four species (*SI Appendix*, Fig. S1). One of these species, *P. carnea*, is a hydra, implying that this counterion evolved early in the evolution of cnidarians. Interestingly, in the only other functional examination of radiate opsins (in those found in the lens-eye–bearing *T. cystophora*), the only opsins that showed functional coupling to G proteins in vitro were those containing E94 (10). Quantifying the link between this unique counterion and the efficiency of G-protein activation could form the basis for finding unique tools for optogenetics from these animals. As an aside, sequence analysis reveals that at least four cnidarian opsins also possess an aspartate or glutamate at position 113 (10). As these opsins also have an equivalent of R186, and our data show that a charged residue at 113 can act as a counterion in JellyOp, it seems likely that Cnidaria also independently evolved the vertebrate counterion location.

Finally, position 94—the third only counterion position in animal opsins—is also of functional significance in other GPCRs. For instance, a T94I mutation in human rhodopsin causes congenital stationary night blindness (37) due to establishment of a direct van der Waals contact with retinal, which weakens the interaction between the Schiff base and the counterion at E113 (38). Furthermore, the equivalent position—2.61x60 in the GPCR numbering scheme (32)—is also involved in ligand recognition in several rhodopsin-like GPCRs, such as the human β_2-adrenergic, A2A adenosine, k-opioid, sphingosine 1-phosphate, and chemokine CXCR4 receptors (39). A sequence analysis across class A GPCRs reveals that several families of peptide receptors (such as human melanocortin receptors) feature a glutamate at this position, which is also involved in ligand binding (40).

Materials and Methods

Spectroscopy. JellyOp and its mutants were expressed and purified as previously described (5). Expressed proteins were reconstituted by adding an excess of 11-*cis*-retinal, extracted with 1% *n*-dodecyl β-D-maltoside (DM) in Hepes buffer (pH 6.5) containing 140 mM NaCl (buffer A) and purified using 1D4-agarose with buffer A containing 0.02% DM. Absorption spectra were measured with a spectrophotometer (UV2450; Shimadzu) at 4 °C.

cAMP Assay and Action Spectrum Generation. JellyOp activation in HEK293 cells was measured using the bioluminescent GloSensor22F reporter as described previously (17, 18). Relative sensitivity was determined from second messenger irradiance response curves at eight near-monochromatic wavelength bands. λ_{max} was determined by fitting with Govardovskii formula nomogram templates [as described (19) and applied to second messenger responses previously (20)]. All light stimuli were delivered using the pe-4000 CoolLED system (CoolLED).

Structural Modeling and Molecular-Dynamics Simulations. A 3D model of JellyOp was built by homology modeling with Modeller, version 9.14 (41), using the crystal structure of squid rhodopsin [PDB ID code 2Z73 (42)] as a template. The model was embedded in a hydrated lipid bilayer, and the entire

system equilibrated using molecular dynamics. The equilibrated system was then used as a starting point to perform unrestrained molecular dynamics simulations. Simulations were carried out with NAMD 2.10 (43, 44).

Phylogenetic Reconstruction of Ancestral Opsin Sequences. The reconstruction of ancestral sequences was performed using the PhyloBot web server (26) (phylobot.com/). Within the PhyloBot server, selected sequences from radiata and bilateria (*SI Appendix*, Table S2) were aligned with MUSCLE (45) and MSAProbs (46) with default settings; the program ProtTest (47) recommended the "PROTGAMMALG" [LG + GAMMA] model of evolution (48); maximum-likelihood trees were built using RAxML (49); PhyML was used to assess the statistical support of the data for the calculated trees (50); and, finally, the ancestral opsin sequences at various internal nodes were reconstructed using the software packages PAML (51) and Lazarus (52). The 3D structure of ancestor A was modeled with Modeller, version 9.14 (41), using squid rhodopsin as a template [PDB ID code 2Z73 (42)] and the sequence alignment obtained in the PhyloBot web server.

Structure-Based Sequence Conservation Analysis. Using the crystal structure of bovine rhodopsin [PDB ID code 1GZM (53)], we selected all residues within 10 Å of the Schiff base (LYS296:NZ) in the retinal binding pocket as potential sites for a counterion. We then measured the sequence variability at these positions in an alignment of ∼900 sequences from a recent large-scale analysis of opsin evolution (23), in which 26 outgroups had been removed.

Full methods can be accessed in *SI Appendix*, *SI Materials and Methods*.

ACKNOWLEDGMENTS. We acknowledge support from Human Frontiers Science Program Grant RGP0034/2014 (to R.J.L., G.F.X.S., and A.T.); Biotechnology and Biological Sciences Research Council Grant BB/K002252/1 (to R.J.L.); Japanese Society for the Promotion of Science KAKENHI Grant 15H05777 (to A.T.); Japanese Science and Technology Agency CREST Grant JPMJCR1753 (to A.T.); Swiss National Science Foundation Grant 173335 and National Centre of Competence in Research "Molecular Ultrafast Science and Technology" Program (to G.F.X.S.); European Community's Seventh Framework Program (FP7/2007-2013) under Grant Agreement 290605 (COFUND: PSI-FELLOW) (to E.M.); and Swiss National Science Foundation Grant CRSII2_160805 and the Swiss National Supercomputing Centre (to X.D.).

1. Terakita A (2005) The opsins. *Genome Biol* 6:213.
2. Airan RD, Thompson KR, Fenno LE, Bernstein H, Deisseroth K (2009) Temporally precise in vivo control of intracellular signalling. *Nature* 458:1025–1029.
3. Sakmar TP, Franke RR, Khorana HG (1991) The role of the retinylidene Schiff base counterion in rhodopsin in determining wavelength absorbance and Schiff base p*K*a. *Proc Natl Acad Sci USA* 88:3079–3083.
4. Ebrey TG (2000) pK_a of the protonated Schiff base of visual pigments. *Methods Enzymol* 315:196–207.
5. Terakita A, Yamashita T, Shichida Y (2000) Highly conserved glutamic acid in the extracellular IV–V loop in rhodopsins acts as the counterion in retinochrome, a member of the rhodopsin family. *Proc Natl Acad Sci USA* 97:14263–14267.
6. Sakmar TP, Franke RR, Khorana HG (1989) Glutamic acid-113 serves as the retinylidene Schiff base counterion in bovine rhodopsin. *Proc Natl Acad Sci USA* 86:8309–8313.
7. Nathans J (1990) Determinants of visual pigment absorbance: Identification of the retinylidene Schiff's base counterion in bovine rhodopsin. *Biochemistry* 29:9746–9752.
8. Zhukovsky EA, Oprian DD (1989) Effect of carboxylic acid side chains on the absorption maximum of visual pigments. *Science* 246:928–930.
9. Tsutsui K, Shichida Y (2010) Multiple functions of Schiff base counterion in rhodopsins. *Photochem Photobiol Sci* 9:1426–1434.
10. Liegertová M, et al. (2015) Cubozoan genome illuminates functional diversification of opsins and photoreceptor evolution. *Sci Rep* 5:11885.
11. Yan ECY, et al. (2003) Retinal counterion switch in the photoactivation of the G protein-coupled receptor rhodopsin. *Proc Natl Acad Sci USA* 100:9262–9267.
12. Nilsson D-E, Gislén L, Coates MM, Skogh C, Garm A (2005) Advanced optics in a jellyfish eye. *Nature* 435:201–205.
13. Garm A, Oskarsson M, Nilsson D-E (2011) Box jellyfish use terrestrial visual cues for navigation. *Curr Biol* 21:798–803.
14. Garm A, O'Connor M, Parkefelt L, Nilsson D-E (2007) Visually guided obstacle avoidance in the box jellyfish *Tripedalia cystophora* and *Chiropsella bronzie*. *J Exp Biol* 210:3616–3623.
15. Garm A, Bielecki J (2008) Swim pacemakers in box jellyfish are modulated by the visual input. *J Comp Physiol A Neuroethol Sens Neural Behav Physiol* 194:641–651.
16. Koyanagi M, et al. (2008) Jellyfish vision starts with cAMP signaling mediated by opsin-G_s cascade. *Proc Natl Acad Sci USA* 105:15576–15580.
17. Bailes HJ, et al. (2017) Optogenetic interrogation reveals separable G-protein-dependent and -independent signalling linking G-protein-coupled receptors to the circadian oscillator. *BMC Biol* 15:40.
18. Bailes HJ, Zhuang L-Y, Lucas RJ (2012) Reproducible and sustained regulation of Gαs signalling using a metazoan opsin as an optogenetic tool. *PLoS One* 7:e30774.
19. Govardovskii VI, Fyhrquist N, Reuter T, Kuzmin DG, Donner K (2000) In search of the visual pigment template. *Vis Neurosci* 17:509–528.
20. Bailes HJ, Lucas RJ (2013) Human melanopsin forms a pigment maximally sensitive to blue light ($\lambda_{max} \approx 479$ nm) supporting activation of $G_{q/11}$ and $G_{i/o}$ signalling cascades. *Proc Biol Sci* 280:20122987.
21. Thornton JW (2004) Resurrecting ancient genes: Experimental analysis of extinct molecules. *Nat Rev Genet* 5:366–375.
22. Feuda R, Hamilton SC, McInerney JO, Pisani D (2012) Metazoan opsin evolution reveals a simple route to animal vision. *Proc Natl Acad Sci USA* 109:18868–18872.
23. Porter ML, et al. (2012) Shedding new light on opsin evolution. *Proc Biol Sci* 279:3–14.
24. Suga H, Schmid V, Gehring WJ (2008) Evolution and functional diversity of jellyfish opsins. *Curr Biol* 18:51–55.
25. Terakita A, et al. (2004) Counterion displacement in the molecular evolution of the rhodopsin family. *Nat Struct Mol Biol* 11:284–289.
26. Hanson-Smith V, Johnson A (2016) PhyloBot: A web portal for automated phylogenetics, ancestral sequence reconstruction, and exploration of mutational trajectories. *PLoS Comput Biol* 12:e1004976.
27. Gumulya Y, Gillam EMJ (2017) Exploring the past and the future of protein evolution with ancestral sequence reconstruction: The "retro" approach to protein engineering. *Biochem J* 474:1–19.
28. Yokoyama S, et al. (2014) Epistatic adaptive evolution of human color vision. *PLoS Genet* 10:e1004884.
29. Katayama K, Nonaka Y, Tsutsui K, Imai H, Kandori H (2017) Spectral tuning mechanism of primate blue-sensitive visual pigment elucidated by FTIR spectroscopy. *Sci Rep* 7:4904.
30. Ota T, Furutani Y, Terakita A, Shichida Y, Kandori H (2006) Structural changes in the Schiff base region of squid rhodopsin upon photoisomerization studied by low-temperature FTIR spectroscopy. *Biochemistry* 45:2845–2851.
31. Tsukamoto H, Farrens DL, Koyanagi M, Terakita A (2009) The magnitude of the light-induced conformational change in different rhodopsins correlates with their ability to activate G proteins. *J Biol Chem* 284:20676–20683.
32. Pándy-Szekeres G, et al. (2018) GPCRdb in 2018: Adding GPCR structure models and ligands. *Nucleic Acids Res* 46:D440–D446.
33. Castiglione GM, et al. (2017) Evolution of nonspectral rhodopsin function at high altitudes. *Proc Natl Acad Sci USA* 114:7385–7390.
34. Blackledge TA, Gillespie RG (2004) Convergent evolution of behavior in an adaptive radiation of Hawaiian web-building spiders. *Proc Natl Acad Sci USA* 101:16228–16233.
35. Yan ECY, et al. (2002) Function of extracellular loop 2 in rhodopsin: Glutamic acid 181 modulates stability and absorption wavelength of metarhodopsin II. *Biochemistry* 41:3620–3627.
36. Kojima K, et al. (2017) Evolutionary steps involving counterion displacement in a tunicate opsin. *Proc Natl Acad Sci USA* 114:6028–6033.
37. al-Jandal N, et al. (1999) A novel mutation within the rhodopsin gene (Thr-94-Ile) causing autosomal dominant congenital stationary night blindness. *Hum Mutat* 13:75–81.
38. Singhal A, et al. (2016) Structural role of the T94I rhodopsin mutation in congenital stationary night blindness. *EMBO Rep* 17:1431–1440.
39. Venkatakrishnan AJ, et al. (2013) Molecular signatures of G-protein-coupled receptors. *Nature* 494:185–194.
40. Yang YK, et al. (2000) Molecular determinants of ligand binding to the human melanocortin-4 receptor. *Biochemistry* 39:14900–14911.
41. Webb B, Sali A (2016) Comparative protein structure modeling using MODELLER. *Curr Protoc Bioinformatics* 54:5.6.1–5.6.37.
42. Murakami M, Kouyama T (2008) Crystal structure of squid rhodopsin. *Nature* 453: 363–367.
43. Phillips JC, et al. (2005) Scalable molecular dynamics with NAMD. *J Comput Chem* 26: 1781–1802.
44. Best RB, et al. (2012) Optimization of the additive CHARMM all-atom protein force field targeting improved sampling of the backbone φ, ψ and side-chain χ(1) and χ(2) dihedral angles. *J Chem Theory Comput* 8:3257–3273.
45. Edgar RC (2004) MUSCLE: Multiple sequence alignment with high accuracy and high throughput. *Nucleic Acids Res* 32:1792–1797.
46. Liu Y, Schmidt B, Maskell DL (2010) MSAProbs: Multiple sequence alignment based on pair hidden Markov models and partition function posterior probabilities. *Bioinformatics* 26:1958–1964.
47. Abascal F, Zardoya R, Posada D (2005) ProtTest: Selection of best-fit models of protein evolution. *Bioinformatics* 21:2104–2105.
48. Le SQ, Gascuel O (2008) An improved general amino acid replacement matrix. *Mol Biol Evol* 25:1307–1320.
49. Stamatakis A (2014) RAxML version 8: A tool for phylogenetic analysis and post-analysis of large phylogenies. *Bioinformatics* 30:1312–1313.
50. Guindon S, et al. (2010) New algorithms and methods to estimate maximum-likelihood phylogenies: Assessing the performance of PhyML 3.0. *Syst Biol* 59:307–321.
51. Yang Z (2007) PAML 4: Phylogenetic analysis by maximum likelihood. *Mol Biol Evol* 24:1586–1591.
52. Hanson-Smith V, Kolaczkowski B, Thornton JW (2010) Robustness of ancestral sequence reconstruction to phylogenetic uncertainty. *Mol Biol Evol* 27:1988–1999.
53. Li J, Edwards PC, Burghammer M, Villa C, Schertler GFX (2004) Structure of bovine rhodopsin in a trigonal crystal form. *J Mol Biol* 343:1409–1438.